

# A novel double-walled Cd(II) metal–organic framework as highly selective luminescent sensor for $\text{Cr}_2\text{O}_7^{2-}$ anion

Yu-Pei Xia<sup>a,c</sup>, Chen-Xue Wang<sup>a,c</sup>, Rui Feng<sup>a,c</sup>, Kai Li<sup>a,c</sup>, Ze Chang<sup>a,c,\*</sup>, Xian-He Bu<sup>a,b,c,\*</sup>

<sup>a</sup> School of Materials Science and Engineering, National Institute for Advanced Materials, Tianjin Key Laboratory of Metal and Molecule-Based Material Chemistry, Nankai University, Tianjin 300350, China

<sup>b</sup> State Key Laboratory of Elemento-Organic Chemistry, College of Chemistry, Nankai University, Tianjin 300071, China

<sup>c</sup> Collaborative Innovation Center of Chemical Science and Engineering (Tianjin), Tianjin 300072, China

## ARTICLE INFO

### Article history:

Received 1 June 2018

Accepted 2 July 2018

Available online 11 July 2018

### Keywords:

Metal–organic framework

Crystal structure

Luminescent sensing

Luminescent sensor

Toxic anion

## ABSTRACT

A novel Cd(II) metal–organic framework,  $[\text{Cd}_3\text{L}_3(\text{DMF})_2]_n$  (**1**), was synthesized using 5-(1H-1,2,4-triazol-1-yl)isophthalic acid ( $\text{H}_2\text{L}$ ) and  $\text{Cd}(\text{NO}_3)_2 \cdot 6\text{H}_2\text{O}$  under solvothermal condition. The structure of **1** was characterized by X-ray crystallography, elemental analysis, and IR spectrum. Compound **1** possessed a fascinating three-dimensional (3D) double-walled framework with one-dimensional (1D) channels. The luminescence properties of compound **1** toward anion detection were systematically investigated. The results indicate that compound **1** behaves as a highly selective and sensitive ‘turn-off’ luminescence probe toward  $\text{Cr}_2\text{O}_7^{2-}$  anion.

© 2018 Elsevier Ltd. All rights reserved.

## 1. Introduction

Metal–organic frameworks (MOFs), which were constructed based on assembly of metal ions and organic bridging ligands, have emerged as a promising class of material in many areas, such as gas storage and separation, luminescence sensing, catalysis and so on [1–5]. A large number of MOFs have been synthesized by using different metal salts and selected organic ligands in the past few decades. Among them, luminescence MOFs have attracted much attentions due to their outstanding sensing properties. On the basis of widely investigations, it has been proved that luminescence metal–organic frameworks can be good chemosensor probes for highly selective and sensitive detection toward harmful cations, anions and organic solvents/vapors/dyes [6–10].

Among the various targeted harmful analysts,  $\text{Cr}_2\text{O}_7^{2-}$  anion has caught much attention as one kind of carcinogen, which is listed as a dangerous pollutant by the U.S. Environmental Protection Agency [4]. The  $\text{Cr}_2\text{O}_7^{2-}$  anion can caused severe harm to the environment and health of human beings, therefore the selective and sensitive sensing of  $\text{Cr}_2\text{O}_7^{2-}$  anion is significant in the aspect

of environment protection. To data, there are only a few luminescence MOFs that reveal highly selective and sensitive sensing toward  $\text{Cr}_2\text{O}_7^{2-}$  anion [11,12]. Therefore, the exploration of luminescence MOFs toward detection of  $\text{Cr}_2\text{O}_7^{2-}$  anion could be a challenging task.

On the other hand, among the various kinds of MOFs constructed with distinct ligands, the ones based on asymmetric carboxylate-*N*-heterocyclic ligand has revealed remarkable performances in luminescent sensing. For example, Xiao-Yu Guo et al. [13] reported a Zn(II)-organic framework for highly selective and sensitive of  $\text{Cr}^{\text{VI}}$  anions based on 5-(2-methylpyridin-4-yl) isophthalic acid ligand. Yu Wu et al. [14] have developed two luminescence Zn/Cd-MOF sensors for detection  $\text{Cr}_2\text{O}_7^{2-}$  based on a semi-flexible asymmetric ligand 4'-(4-(3,5-dicarboxyphenoxy) phenyl)-4,2':6',4''-terpyridine. Inspired by these relevant works, we selected a new asymmetric ligand, 5-(1H-1,2,4-triazol-1-yl) isophthalic acid ( $\text{H}_2\text{L}$ ), for the construction of functional MOFs. Herein, we report the synthesis, structure, and luminescent sensing property of a novel Cd(II)-based MOF, namely  $[\text{Cd}_3\text{L}_3(\text{DMF})_2]_n$  (**1**) (DMF = *N,N*-dimethylformamide), which features fascinating double-walled three dimensional (3D) framework structure [15]. Topology analysis reveals that compound **1** possesses a novel 3,9-c net **gfy** topology. Remarkably, the luminescence sensing investigation indicates that **1** exhibit highly selective and sensitive sensing toward  $\text{Cr}_2\text{O}_7^{2-}$  anion. In addition, the sensing mechanism of **1** was discussed.

\* Corresponding authors at: School of Materials Science and Engineering, National Institute for Advanced Materials, Tianjin Key Laboratory of Metal and Molecule-Based Material Chemistry, Nankai University, Tianjin 300350, China.

E-mail addresses: [changze@nankai.edu.cn](mailto:changze@nankai.edu.cn) (Z. Chang), [buxh@nankai.edu.cn](mailto:buxh@nankai.edu.cn) (X.-H. Bu).

## 2. Experimental

### 2.1. Materials and methods

Organic solvents and  $\text{Cd}(\text{NO}_3)_2 \cdot 6\text{H}_2\text{O}$  were purchased from Aladdin company and used as received without further purification. The  $\text{H}_2\text{L}$  is also commercial available.  $^1\text{H}$  NMR spectrum of ligand  $\text{H}_2\text{L}$  was measured on a Bruker 400 M ( $d_6$ -DMSO). Elemental analyses (C, H, and N) were performed with a Vario EL cube analyzer. FT-IR spectra were measured on a Bruker Tensor 37 spectrophotometer with anhydrous KBr pellets in the region of 4000–400  $\text{cm}^{-1}$ . The UV–Vis spectra were recorded on a Shimadzu UV-2600 spectrometer. The photoluminescence (PL) spectra were measured on a Hitachi F4500 luminescence spectrometer. The Powder X-ray diffraction (PXRD) patterns were collected at the  $2\theta$  range from  $3^\circ$  to  $55^\circ$  on a Rigaku D/Max-2500 with  $\text{Cu K}\alpha$  radiation at room temperature. Thermalgravimetric analysis (TGA) were measured on a Rigaku TG8121 thermoanalyzer from room temperature to  $800^\circ\text{C}$  with a heating rate at  $10^\circ\text{C min}^{-1}$ . Simulated PXRD pattern was obtained by the CIF file and Mercury software [16] (version: 3.10).

### 2.2. Synthesis of $[\text{Cd}_3\text{L}_3(\text{DMF})_2]_n$ (**1**)

A mixture of  $\text{Cd}(\text{NO}_3)_2 \cdot 6\text{H}_2\text{O}$  (0.0154 g, 0.05 mmol),  $\text{H}_2\text{L}$  (0.0058 g, 0.025 mmol) and  $\text{DMF}/\text{CH}_3\text{CN}$  (7 mL, 4:3, V/V) was placed in a 10 mL vial and ultrasonic until a clear solution was obtained. Then the vial was capped and heated at  $85^\circ\text{C}$  for 2 days and cooled to room temperature at a rate of  $10^\circ\text{C/h}$ . Colorless plank shaped crystals of **1** were isolated by filtration and collected in 42% yield (based on Cd). The resulting crystals were rinsed with DMF three times and then dried at room temperature. Elemental analysis for  $\text{C}_{36}\text{H}_{29}\text{Cd}_3\text{N}_{11}\text{O}_{14}$  (**1**): calcd: C, 36.74; H, 2.48; N, 13.09; found: C, 36.67; H, 2.51; N 13.15%.

### 2.3. X-ray crystallography

A suitable crystal of **1** was selected for X-ray single crystal diffraction test and the data was collected on a Rigaku XtaLAB MM007 CCD diffractometer with  $\text{Cu K}\alpha$  radiation ( $\lambda = 1.5418 \text{ \AA}$ ) radiation. The crystal was kept at 100 K using nitrogen flow during the data collection. The CrystalAlice PRO program was used to

integrate the diffraction profiles. The final structure was solved by SHELXT [17] and refined by full-matrix least-square methods with the SHELXL [18] program. All non-hydrogen atoms were refined with anisotropic displacement parameters, while the hydrogen atoms on ligands were placed in idealized positions with isotropic thermal parameters. Full crystallographic data for **1** was summarized in Table 1.

## 3. Results and discussion

### 3.1. Description of crystal structure

Single-crystal X-ray diffraction analysis reveals that compound **1** crystallized in the triclinic system with the space group  $P\bar{1}$  and has a 3D double-walled framework. The asymmetric unit of **1** contains three crystallographically independent  $\text{Cd}(\text{II})$  ions, three deprotonated  $\text{L}^{2-}$  ligands and two coordinated DMF molecules (Fig. S3). The three different  $\text{Cd}(\text{II})$  centers demonstrate three different coordination environments. As illustrated in Fig. 1a, The Cd1 center is six coordinated with four carboxylate oxygen atoms from three different  $\text{L}^{2-}$  ligands and two nitrogen atoms from other two  $\text{L}^{2-}$  ligands. The Cd2 center is six coordinated with five carboxylate oxygen atoms from four different  $\text{L}^{2-}$  ligands and one oxygen atom derived from one solvent DMF molecule. The Cd3 center is also six coordinated by four carboxylate oxygen atoms from three different  $\text{L}^{2-}$  ligands, one nitrogen atom derived from another  $\text{L}^{2-}$  ligand, and one oxygen atom from one solvent DMF molecule. In compound **1**, the carboxylic groups of the  $\text{L}^{2-}$  ligand displays three different coordination modes,  $\eta^2$ ,  $\mu_2$ - $\eta^2$ :  $\eta^1$  and  $\mu_2$ - $\eta^1$ :  $\eta^1$  (Fig. 1b). The carboxylic oxygen atoms and the oxygen atoms from the solvent DMF molecules bridged the  $\text{Cd}(\text{II})$  ions to generate indefinitely 1D chain (along  $a$  axis). These chains are further linked by the uncoordinated nitrogen atoms and  $\text{Cd}(\text{II})$  ions to form a novel 3D double-walled structure with 1D channels (Fig. 1c). The Cd-O and Cd-N bonds distances are all distributed in the normal range of 2.225(7)–2.528(7)  $\text{\AA}$ , which are comparable with other  $\text{Cd}(\text{II})$ -MOFs [19–21]. The selected bond lengths are listed in Table S1. The double-walled structure of **1** aroused our enormous interests, so the ToposPro software [22] was used to analyze the topology structure in order to better understand the framework structure of **1**. Based on the above descriptions, the 3D framework of **1** can simplified as a novel 3,9-c gfy network, with a point symbol of  $\{4^{12}.6^{15}.8^9\}\{4^3\}_3$  (Fig. 1d). To the best of our knowledge, this topology type is uncommon in MOFs [23,24]. The potentially free volume (with the coordinated DMF molecules) of compound **1** is 24.1% ( $2492.6 \text{ \AA}^3$  per unit cell volume), calculated by the PLATON software [25].

### 3.2. Purity and thermal stability

The phase purity of bulk sample of **1** was checked by the powder X-ray diffraction (PXRD). As shown in Fig. 2a, the observed pattern of **1** matched well with the simulated one which was generated by the Mercury software. This result demonstrating that the bulk sample possessed high phase purity. The thermal gravimetric analysis (TGA) of **1** was tested under an air atmosphere. The weight loss before  $350^\circ\text{C}$  can be attributed to the loss of the surface and coordinated DMF molecules (Fig. 2b). Then the sharp fall of profile to about 23% at about  $450^\circ\text{C}$  indicated the decomposition of the compound, and the plateau at higher temperature can be ascribed to the corresponding oxide.

**Table 1**  
Crystal data and structure refinement parameters of **1**.

Compound	<b>1</b>
Empirical formula	$\text{C}_{36}\text{H}_{29}\text{Cd}_3\text{N}_{11}\text{O}_{14}$
Formula weight	1176.90
$T$ (K)	100
Crystal system	triclinic
Space group	$P\bar{1}$
Radiation	$\text{Cu K}\alpha$ ( $\lambda = 1.54184$ )
$a$ ( $\text{\AA}$ )	10.3502(3)
$b$ ( $\text{\AA}$ )	15.0971(3)
$c$ ( $\text{\AA}$ )	17.5247(6)
$\alpha$ ( $^\circ$ )	108.717(3)
$\beta$ ( $^\circ$ )	103.082(3)
$\gamma$ ( $^\circ$ )	94.440(2)
$V$ ( $\text{\AA}^3$ )	2492.61(13)
$Z$	2
$D_{\text{calc}}$ ( $\text{g/cm}^3$ )	1.568
Goodness-of-fit on $F^2$ (GOF)	1.047
Final $R$ indexes [ $I \geq 2\sigma(I)$ ]	$R_1 = 0.0818$ , $wR_2 = 0.2274$
Final $R$ indexes [all data]	$R_1 = 0.0843$ , $wR_2 = 0.2297$

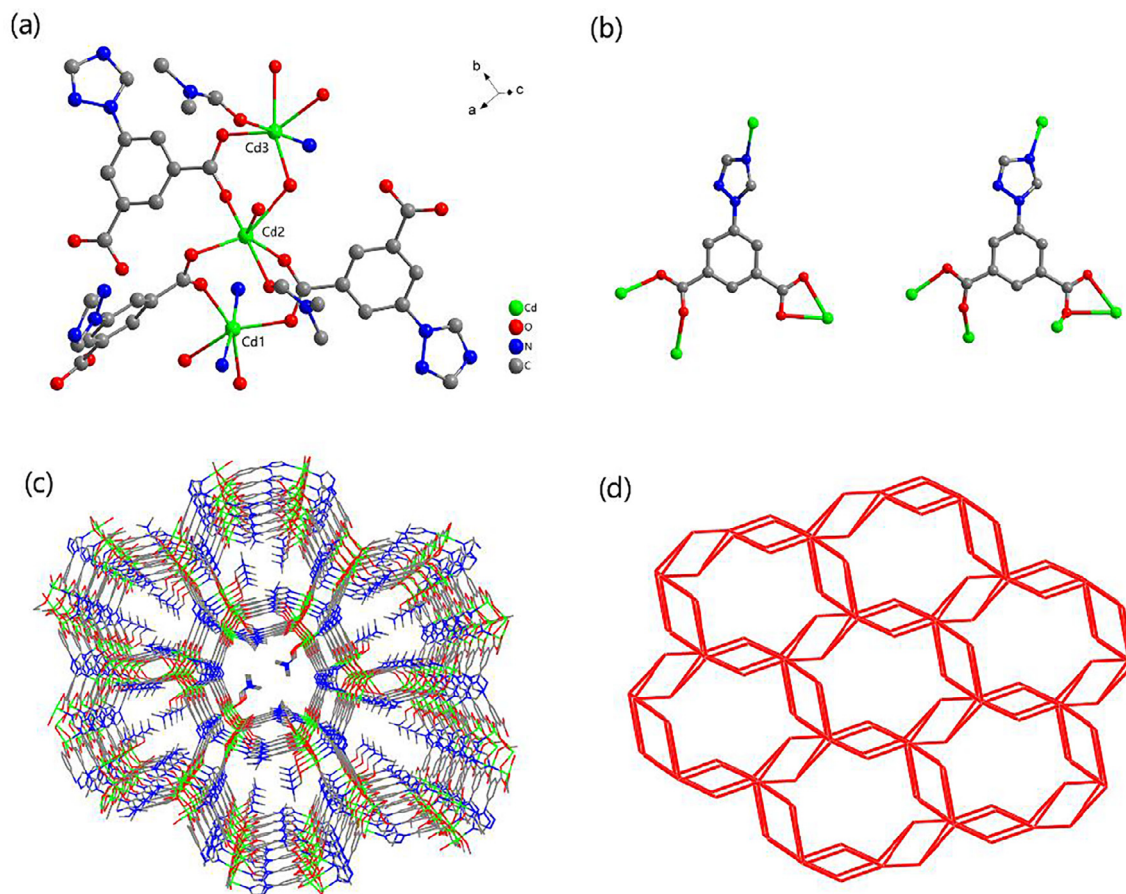


**Fig. 1.** (a) The coordination environments of Cd(II) centers in compound **1**; (b) The coordination modes of the deprotonated  $L^{2-}$  ligands; (c) The 3D framework structure of **1** (along  $a$  axis); (d) Schematic view of the topology of the 3D MOF. Color codes: Cd (green), C (gray), O (red), N (dark blue), H-atoms are omitted for clarity. (Colour online.)

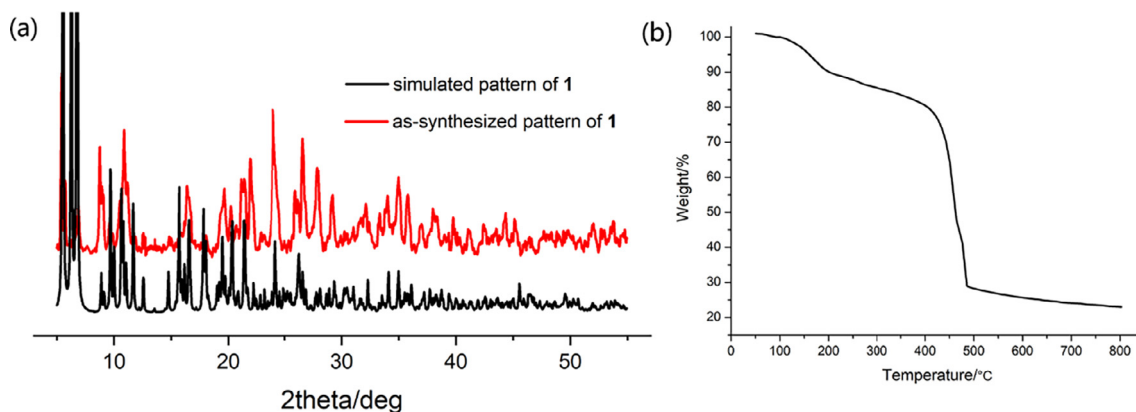


**Fig. 2.** (a) Simulated and as-synthesized PXRD patterns of **1**; (b) TGA profile of **1**.

### 3.3. Luminescence properties

The luminescence properties of  $H_2L$  and **1** in solid state were studied at room temperature (Fig. 3 and Fig. S4). The emission of the free  $H_2L$  centered at 350 nm ( $\lambda_{ex}$  = 300 nm) can be attributed to the  $\pi \rightarrow \pi^*$  or  $\pi \rightarrow n^*$  electronic transitions of the ligand [26–28]. In contrast to that, compound **1** exhibits a strong emission band at 430 nm ( $\lambda_{ex}$  = 331 nm). Since the  $d^{10}$  configuration of Cd(II)

ions is difficult to be oxidized or reduced, the shift of emission shall not be due to the LMCT or MLCT [29,30]. Then the red shifted emission of compound **1** compared to that of the free ligands might be attributed to the packing of the ligand in the framework. The relative intense emission of **1** can be assigned to the chelating and/or bridging influence of metal ions and  $L^{2-}$  ligands, which could significantly increase the robustness of the framework and reduce the energy loss through non-radiative pathways.

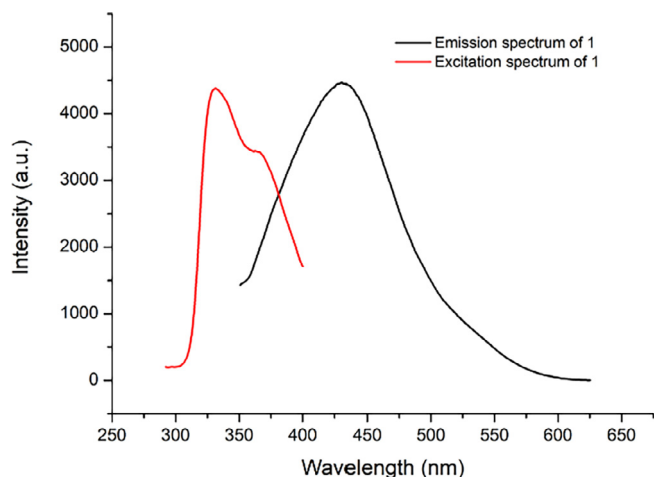


Fig. 3. The solid-state excitation and emission spectra of **1**.

### 3.4. Sensing of $\text{Cr}_2\text{O}_7^{2-}$

On the basis of the emission property of **1**, further experiments were performed to investigate its potential as a luminescent probe toward anions. Finely grind sample of **1** (3 mg) was dispersed in 3 mL of DMF solution, different sodium salt solutions ( $\text{NaX}$  or  $\text{Na}_2\text{X}$ ,  $\text{X} = \text{F}^-$ ,  $\text{Cl}^-$ ,  $\text{Br}^-$ ,  $\text{I}^-$ ,  $\text{C}_2\text{O}_4^{2-}$ ,  $\text{NO}_3^-$ ,  $\text{NO}_2^-$ ,  $\text{SO}_4^{2-}$ ,  $\text{ClO}_4^-$ ,  $\text{Cr}_2\text{O}_7^{2-}$ ) were added in the suspension, respectively. The suspensions were sonicated for 1 h before the following luminescence testing. As shown in Fig. 4a, the emission intensity of the suspension significantly reduced upon the addition of  $\text{Cr}_2\text{O}_7^{2-}$ , while other anions have little impact on the emission intensity of **1**. This result indicating that **1** may be a selective sensor toward  $\text{Cr}_2\text{O}_7^{2-}$  anion. For better understand of the quenching phenomenon, concentration-dependent luminescence studies of  $\text{Cr}_2\text{O}_7^{2-}$  anion on **1** were carried out (Fig. S6). The results show that the luminescence intensities of **1** decreased with the increased concentration of  $\text{Cr}_2\text{O}_7^{2-}$  anion. In the low range of concentrations, the linear relation of the quenching effect was fitted by the Stern–Volmer (SV) equation:

$I_0/I = 1 + K_{\text{sv}}[\text{M}]$  (Fig. 4b). The symbol  $I_0$  and  $I$  mean the luminescence intensities of compound **1** without and with  $\text{Cr}_2\text{O}_7^{2-}$ , while  $[\text{M}]$  is the concentration of  $\text{Cr}_2\text{O}_7^{2-}$  anions. The quenching constant ( $K_{\text{sv}}$ ) is determined to be  $1.2 \times 10^4 \text{ M}^{-1}$  ( $R^2 = 0.99628$ ), which is in the normal range of MOFs based sensors [31–34]. The limit of detection (LOD) of **1** is toward  $\text{Cr}_2\text{O}_7^{2-}$  is determined to be  $3.4 \mu\text{M}$  ( $S/N = 3$ ), indicating a considerable sensing sensitivity of **1** toward  $\text{Cr}_2\text{O}_7^{2-}$  anion.

On the basis of previous research and reports, the luminescence quenching of MOF toward analytes are mainly ascribed to three reasons: (1) the decomposition of the MOF; (2) the competition absorption of the analyte and MOF; (3) energy transfer from the MOF framework to analyte. For better understanding of the sensing behavior of **1** toward  $\text{Cr}_2\text{O}_7^{2-}$ , further experiments were performed for mechanism determination. PXRD test of the MOF sample after sensing experiments revealed that the crystallinity of the sample is well retained (Fig. S7). Therefore, the quenching of the emission was not caused by the decomposition of the framework. On the other hand, the UV–vis spectra of the  $\text{Cr}_2\text{O}_7^{2-}$  solution (Fig. S8) show that there are two broad absorption bands (250–525 nm), while no obvious absorption could be observed in this range for other anions. It is evident that the absorption bands of  $\text{Cr}_2\text{O}_7^{2-}$  overlaps both the excitation and emission bands of compound **1**, which indicates effective absorption competition and energy transfer between **1** and  $\text{Cr}_2\text{O}_7^{2-}$ . Therefore, the sensitive emission quenching of **1** toward  $\text{Cr}_2\text{O}_7^{2-}$  anion can be tentatively attributed to the competition absorption and energy transfer mechanism [35–37].

## 4. Conclusions

In summary, we have successfully synthesized a novel 3D Cd(II) MOF (**1**) using 5-(1H-1,2,4-triazol-1-yl)isophthalic acid ( $\text{H}_2\text{L}$ ) under solvothermal condition. Compound **1** displays an fascinating double-walled 3D framework structure with 1D channels, which could be simplified as a novel 3,9-connected **gfy** topology network. The intense luminescence of **1** could be selectively and sensitively quenched by the presence of  $\text{Cr}_2\text{O}_7^{2-}$  anion, which make **1** a promising sensor of  $\text{Cr}_2\text{O}_7^{2-}$  anion.

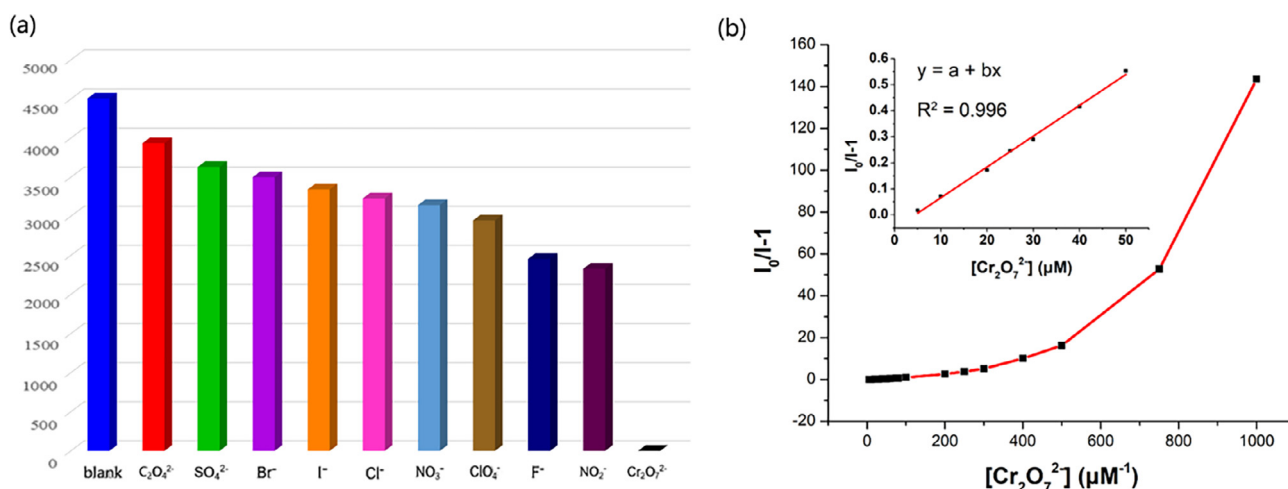


Fig. 4. (a) The luminescent quenching of compound **1** toward different anions. (b) Luminescence quenching effect of **1** upon different concentrations of  $\text{Cr}_2\text{O}_7^{2-}$ .



## Acknowledgements

This work was supported by the NSFC (21371102, 21421001, 21531005, and 21673120), MOE Innovation Team of China (IRT\_17R57), and Natural Science Fund of Tianjin, China (16JCZDJC36900).

## Conflict of interest

The authors declare no competing financial interest.

## Appendix A. Supplementary data

CCDC 1844328 contains the supplementary crystallographic data for compound **1**. These data can be obtained free of charge via <http://www.ccdc.cam.ac.uk/conts/retrieving.html>, or from the Cambridge Crystallographic Data Centre, 12 Union Road, Cambridge CB2 1EZ, UK; fax: (+44) 1223-336-033; or e-mail: [deposit@ccdc.cam.ac.uk](mailto:deposit@ccdc.cam.ac.uk).

Supplementary data associated with this article can be found, in the online version, at <https://doi.org/10.1016/j.poly.2018.07.001>.

## References

- [1] N.S. Bobbitt, M.L. Mendonca, A.J. Howarth, T. Islamoglu, J.T. Hupp, O.K. Farha, R. Q. Snurr, *Chem. Soc. Rev.* 46 (2017) 3357.
- [2] M. Mon, R. Bruno, J. Ferrando-Soria, D. Armentano, E. Pardo, *J. Mater. Chem. A* 6 (2018) 4912.
- [3] W.P. Lustig, S. Mukherjee, N.D. Rudd, A.V. Desai, J. Li, S.K. Ghosh, *Chem. Soc. Rev.* 46 (2017) 3242.
- [4] M. Wu, S. Janssen, *Environ. Sci. Technol.* 45 (2011) 366.
- [5] H.L. Jiang, Q. Xu, *Chem. Commun.* 47 (2011) 3351.
- [6] J. Zhang, L. Zhao, Y. Liu, M. Li, G. Li, X. Meng, *New J. Chem.* 42 (2018) 6839.
- [7] F. Huang, Z. Yang, P. Yao, Q. Yu, J. Tian, H. Bian, S. Yan, D. Liao, P. Cheng, *CrystEngComm* 15 (2013) 2657.
- [8] Y. Liu, L. Liu, X. Zhang, J. Wu, *J. Mol. Struct.* 1156 (2018) 583.
- [9] M.D. Allendorf, C.A. Bauer, R.K. Bhakta, R.J.T. Houk, *Chem. Soc. Rev.* 38 (2009) 1330.
- [10] J. Ma, L. Chen, M. Wu, S. Zhang, K. Xiong, D. Han, F. Jiang, M. Hong, *CrystEngComm* 15 (2013) 911.
- [11] T. Song, J. Dong, H. Gao, J. Cui, B. Zhao, *Dalton Trans.* 46 (2017) 13862.
- [12] Z. Yao, G. Li, J. Xu, T. Hu, X. Bu, *Chem.-Eur. J.* 24 (2018) 3192.
- [13] X. Guo, F. Zhao, J. Liu, Z. Liu, Y. Wang, *J. Mater. Chem. A* 5 (2017) 20035.
- [14] Y. Wu, J. Wu, Z. Luo, J. Wang, Y. Li, Y. Han, J. Liu, *Rsc. Adv.* 7 (2017) 10415.
- [15] D. Tian, Q. Chen, Y. Li, Y. Zhang, Z. Chang, X. Bu, *Angew. Chem. Int. Ed.* 53 (2014) 837.
- [16] C.F. Macrae, P.R. Edgington, P. McCabe, E. Pidcock, G.P. Shields, R. Taylor, M. Towler, J. van de Streek, *J. Appl. Crystallogr.* 39 (2006) 453.
- [17] G.M. Sheldrick, *Acta Crystallogr. A* 71 (2015) 3.
- [18] G.M. Sheldrick, *Acta Crystallogr. C* 71 (2015) 3.
- [19] Q. Cheng, X. Han, Y. Tong, C. Huang, J. Ding, H. Hou, *Inorg. Chem.* 56 (2017) 1696.
- [20] F. Yuan, Y. Yuan, M. Chao, D.J. Young, W. Zhang, J. Lang, *Inorg. Chem.* 56 (2017) 6522.
- [21] S. Chand, S.M. Elahi, A. Pal, M.C. Das, *Dalton Trans.* 46 (2017) 9901.
- [22] V.A. Blatov, A.P. Shevchenko, D.M. Proserpio, *Cryst. Growth Des.* 14 (2014) 3576.
- [23] F. Wang, X. Wu, R. Yu, C. Lu, *Inorg. Chem. Commun.* 17 (2012) 169.
- [24] Z. Xu, L.L. Han, G.L. Zhuang, J. Bai, D. Sun, *Inorg. Chem.* 54 (2015) 4737.
- [25] A.L. Spek, *Acta Crystallogr. D* 65 (2009) 148.
- [26] J. Hao, B. Yan, *Chem. Commun.* 51 (2015) 7737.
- [27] D. Wang, L. Zhang, G. Li, Q. Huo, Y. Liu, *Rsc. Adv.* 5 (2015) 18087.
- [28] Q. Xu, J. Ge, Q. Zhou, J. Lu, S. Ji, L. Wang, Y. Zhang, X. Jin, B. Wu, *Dalton Trans.* 40 (2011) 2805.
- [29] J. Jin, J. Wu, Y. He, B. Li, J. Liu, R. Prasad, A. Kumar, S.R. Batten, *CrystEngComm* 19 (2017) 6464.
- [30] F. Yi, M. Gu, S. Wang, J. Zheng, L. Pan, L. Han, *Inorg. Chem.* 57 (2018) 2654.
- [31] S. Chen, Z. Shi, L. Qin, H. Jia, H. Zheng, *Cryst. Growth Des.* 17 (2017) 67.
- [32] Y. Zhang, V.A. Blatov, T. Zheng, C. Yang, L. Qian, K. Li, B. Li, B. Wu, *Dalton Trans.* 47 (2018) 6189.
- [33] Y. Yang, F. Qiu, C. Xu, Y. Feng, G. Zhang, W. Liu, *Dalton Trans.* (2018).
- [34] F. Yi, S. Wang, M. Gu, J. Zheng, L. Han, *J. Mater. Chem. C* 6 (2018) 2010.
- [35] R. Lv, J. Wang, Y. Zhang, H. Li, L. Yang, S. Liao, W. Gu, X. Liu, *J. Mater. Chem. A* 4 (2016) 15494.
- [36] Y. Ning, L. Wang, G. Yang, Y. Wu, N. Bai, W. Zhang, Y. Wang, *Dalton Trans.* 45 (2016) 12800.
- [37] W. Liu, X. Huang, C. Xu, C. Chen, L. Yang, W. Dou, W. Chen, H. Yang, W. Liu, *Chem.-Eur. J.* 22 (2016) 18769.